Available online at www.sciencedirect.com

ScienceDirect

Ceramics International 40 (2014) 1519–1524

CERAMICS INTERNATIONAL

www.elsevier.com/locate/ceramint

Facile co-precipitation synthesis of shape-controlled magnetite nanoparticles

Lazhen Shen, Yongsheng Qiao, Yong Guo*, Shuangming Meng, Guochen Yang, Meixia Wu, Jianguo Zhao

School of Chemistry and Chemical Engineering, Shanxi Datong University, Datong 037009, P R China

Received 7 May 2013; received in revised form 8 July 2013; accepted 8 July 2013
Available online 15 July 2013

Abstract

Monodispersed magnetite (Fe_3O_4) nanoparticles with high saturation magnetization, including nanospheres, nanoneedles and nanocubes, were synthesized by the co-precipitation method. The shape of magnetite nanoparticles was controlled by changing the amount of sodium dodecyl sulfate (SDS) and the particle size was adjusted by the irradiation time of visible light. The Fe_3O_4 nanospheres, nanoneedles and nanocubes were obtained with the addition of 0 g, 0.1–0.4 g and 0.5–1.0 g SDS, respectively. The particle size of nanospheres, nanoneedles and nanocubes of magnetite was ~15 nm, 100×12 nm^2 (length × width) and ~50 nm under the irradiation time of 30 min. The phase structure, particle shape and size of the samples were characterized by transmission electron microscopy (TEM), X-ray diffraction (XRD) and Fourier transform infrared spectroscopy (FTIR). The as-prepared magnetite nanoparticles from TEM images exhibited a high level of crystallinity with narrow size distribution and good dispersion. The XRD results showed that all the magnetite nanoparticles were pure Fe_3O_4 phase with obvious diffraction peaks. The products exhibited the attractive magnetic properties with high saturation magnetization, which were examined by a vibrating sample magnetometer (VSM).

Keywords: Magnetite; Nanoparticles; Shape-controlled; Saturation magnetization; Visible light irradiation

1. Introduction

Magnetite (Fe_3O_4) exhibits the unique electric and magnetic properties based on the transfer of electrons between Fe^{2+} and Fe^{3+} in the cubic sites [1]. Due to the unique properties and advantages of magnetite, such as strong magnetism, good biocompatibility, long durability, low toxicity and low cost [2,3], it is widely used in magnetic biomedicine [4–6], heavy metal ions removal [7,8], electromagnetic wave absorption [9] and other fields [10–12]. These properties of magnetite strongly depend on their dimension, shape, saturation magnetization as well as monodispersion [13,14].

Many research groups have worked to synthesize magnetite nanospheres, nanocubes, nanoneedles and nanoporous particles by hydrothermal methods [15], co-precipitation methods [16] solvothermal methods [17,18], sonochemical methods [13] and self-assembly methods [19]. These studies provided many useful preparation technologies for the preparation of Fe_3O_4 with different shapes. However, most of Fe_3O_4 nanoparticles obtained by the co-precipitation method are spherical shaped. For instance, the magnetite nanospheres have been synthesized using the co-precipitation method, but the hexanoic acid and loeic acid were employed as the coating agents during the initial crystallization phase of the magnetite [20]. These organic acids are expensive reagents and not environment friendly, and the products obtained have wide particle size distribution of 10–40 nm and small saturation magnetization of 58.72 emu/g. The various methods have been applied to synthesize the nanocubes, nanoplates, nanoneedles or nanorods of magnetite using a solvothermal method [17], hydrothermal method [21], and template method [22] rather than the co-precipitation method. In recent years, Gao et al. have synthesized Fe_3O_4 nanocubes using the solvothermal method at 260 °C in the presence of oleic acid and oleylmine [17].

*Corresponding author. Tel.: +86 352 609 0032.
E-mail address: ybsy_guo@163.com (Y. Guo).

0272-8842/$ - see front matter © 2013 Elsevier Ltd and Techna Group S.r.l. All rights reserved.
http://dx.doi.org/10.1016/j.ceramint.2013.07.037

A series of Fe_3O_4 morphologies (nanorods, nanoctahedrons and nanocubes) were synthesized via a hydrothermal process [21]. Zheng et al. have prepared different morphologies of Fe_3O_4 nanostructures, including spherical, cubic, rod-like, and dendritic nanostructure, using polyethylene glycol as a template [22].

In this study, a simple and efficient one-step co-precipitation method is reported to synthesize the shape-controlled magnetite nanoparticles using $FeSO_4$ and $Fe_2(SO_4)_3$ as reactants at room temperature. In order to improve the shape-dependent functional properties, such as electric property and magnetism, the relation between technological parameters and the shape of products were investigated in this paper. Different nanostructures and particle sizes of Fe_3O_4 nanoshperes, nanocubes and nanoneedles were successfully synthesized by carefully controlling the amount of SDS and the time of irradiation with visible light. The crystalline structure, shape and size of the as-obtained Fe_3O_4 nanoparticles were characterized by XRD and TEM technique and the magnetic properties were investigated by VSM at room temperature. The results show that the shape-controlled Fe_3O_4 nanoparticles exhibit strong monodispersity and high saturation magnetization.

2. Experimental

2.1. Characterization

A BDX-3300 model JEOL 100CX-II transmission electron microscope (TEM) was used to carry out the TEM measurements to investigate the morphology and size of magnetite nanoparticles at an accelerating voltage of 200 kV. The obtained samples were characterized on a BDX-3300 diffractometer using CuKα radiation (wavelength, $\lambda = 1.5406$ Å) with variable slits at 45 kV/40 mA to obtain X-ray powder diffraction (XRD) patterns. The structural properties of the samples were determined by using a NEXUS 870 Fourier transform infrared spectroscopy (FTIR) from 450 cm^{-1} to 2000 cm^{-1}. The magnetic measurement of the products was carried out in a USA LDJ 9600-1 vibrating sample magnetometer (VSM). Magnetic hysteresis loops were recorded at room temperature in a field of 10,000 Oe to determine the saturation magnetization (M_s) for the samples.

2.2. Preparation of magnetite nanoparticles

In the typical synthesis, 2.8 g of $FeSO_4 \cdot 7H_2O$ and 4.0 g of $Fe_2(SO_4)_3$ were dissolved in 100 mL distilled water for 5 min using a magnetic stirrer in a 250 mL beaker. Different amounts (0–1.0 g) of sodium dodecyl sulfate (SDS) were added to this solution under stirring. The pH value of the mixture was adjusted to 12 by solid NaOH with stirring for 20 min at room temperature. The visible light was generated by a lamp. The wavelength of the visible light was about 400–750 nm. The reactor was placed at a fixed distance of 10 cm from the lamp for 0–60 min. The black precipitates were formed and then were washed several times with distilled water and ethanol in turn until the pH was neutral. Finally, the resultant black precipitates were dried in air at room temperature to obtain magnetite nanoparticles. The magnetite nanoparticles obtained at different SDS concentrations and visible light time were nanoshperes, nanocubes and nanoneedles.

3. Results and discussion

3.1. TEM results

Different shaped magnetite nanoparticles were prepared by the facile co-precipitation method in the presence of SDS. The experimentations have been performed by adjusting the amount of SDS and the irradiation time of the visible light to investigate their influence on the shape and particle size of magnetite nanoparticles. The nanospheres, nanoneedles and nanocubes of magnetite were synthesized, and the TEM images of the as-prepared Fe_3O_4 are given in Fig. 1. It could be observed that all of the three synthesized Fe_3O_4 nanoparticles displayed a relatively narrow particle size distribution, good dispersion and a perfect and uniform morphology with distinct crystalline structure. Without SDS, the prepared Fe_3O_4 nanoparticles were nanospheres with monodispersion under the visible light irradiation time of 0–60 min. The particle size of magnetite nanospheres could be controlled by increasing the visible light irradiation time. As the irradiation time of the visible light increased from 30 min to 60 min, the size of the as-prepared magnetite nanospheres increased from ~15 nm to ~50 nm as shown in Fig. 1a and b. The Fe_3O_4 nanoneedles could be produced when 0.1–0.4 g SDS was added. As seen from Fig. 1c, the monodispersible Fe_3O_4 nanoneedles were obtained by adding 0.4 g SDS under the visible light irradiation time of 30 min. Under the visible light irradiation time of 60 min, the Fe_3O_4 nanoneedles were prepared with the addition of 0.3 g SDS as shown in Fig. 1d. Furthermore, the diameter of magnetite nanoneedles increased from 100×12 to 115×14 nm (length × width) with the visible light irradiation time increasing from 30 min to 60 min. With the addition of 0.5–1.0 g SDS, the shape of magnetite nanostructures changed from nanoneedles to nanocubes. As shown in Fig. 1e and f, the Fe_3O_4 nanocubes were prepared by adding 0.8 g and 1.0 g SDS, respectively. Similarly, the particle size of the as-obtained Fe_3O_4 nanocubes increased from about 50 nm to about 100 nm with the increase of the irradiation time from 30 min to 60 min. It can be inferred from Fig. 1 that the particle shape of magnetite is controlled by adjusting the SDS amount, and the particle size increases with the increase of the visible light irradiation time. In fact, the visible light irradiation will not influence the particle shape but the particle size and crystalline structure. The reason may be that the visible light irradiation is favorable to the growth of grain. Therefore, the longer the irradiation time of visible light, the larger the particle size, the better the crystallinity of Fe_3O_4 nanoparticles. The particle size is small but with poor crystalline structure without visible light irradiation.

3.2. XRD results

The phase and crystallinity of magnetite nanospheres, nanoneedles and nanocubes prepared at visible light irradiation time of 30 min were investigated using the XRD technique and the results are given in Fig. 2. The XRD patterns indicated that all of the

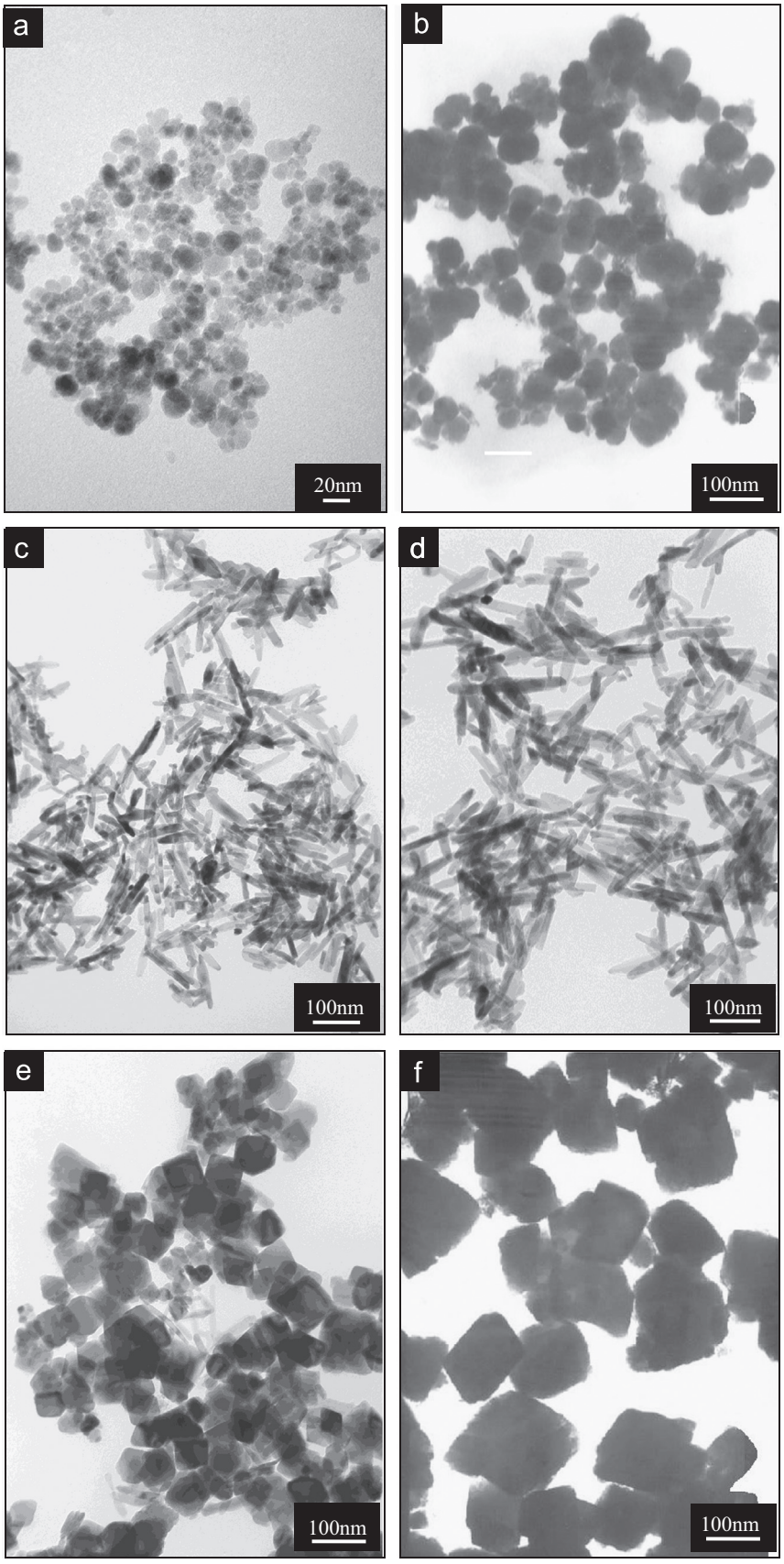

Fig. 1. TEM images of (a, b) nanospheres, (c, d) nanoneedles and (e, f) nanocubes of magnetite obtained at different irradiation times of visible light: (a, c, e) 30 min, and (b, d, f) 60 min and different SDS amounts of 0 g (a, b), 0.4 g (c), 0.3 g (d), 0.8 g (e) and 1.0 g (f).

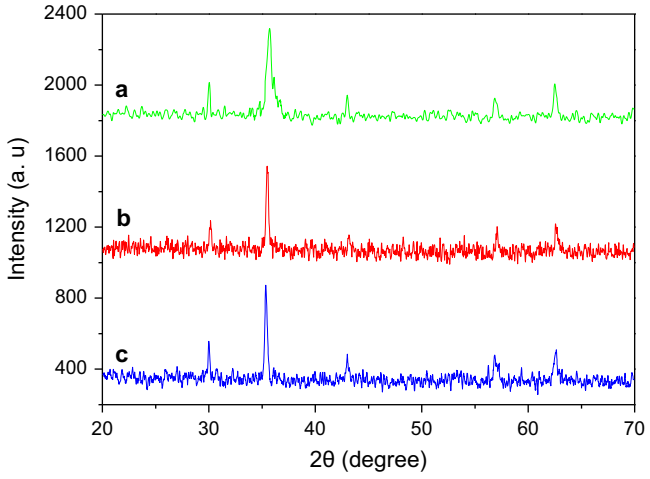

Fig. 2. XRD patterns of (a) nanospheres, (b) nanoneedles and (c) nanocubes of magnetite obtained at the visible light irradiation time of 30 min.

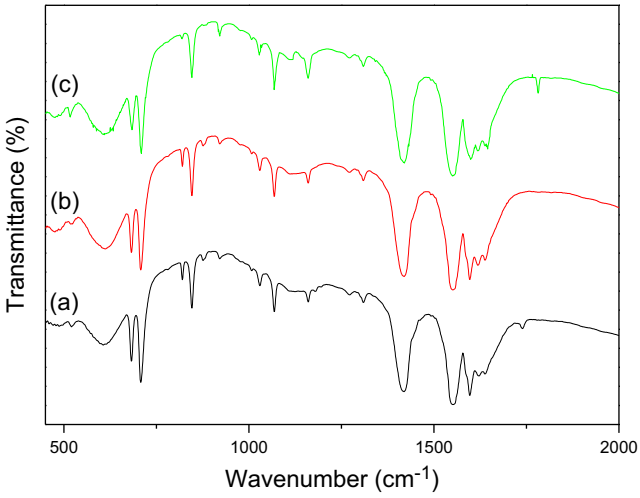

Fig. 3. FTIR spectra of (a) nanospheres, (b) nanoneedles and (c) nanocubes of magnetite obtained at the visible light irradiation time of 30 min.

samples had five obvious diffraction peaks at 2θ of 30.1, 35.4, 42.9, 57.5 and 62.7, representing corresponding indices (220), (311), (400), (511) and (440) of magnetite, respectively [13,23]. The position and relative intensity of all diffraction peaks matched well with the standard of the Fe_3O_4 reflections. No other impurity phase was observed from Fig. 2a–c, indicating the as-synthesized magnetite nanospheres, nanoneedles and nanocubes were pure Fe_3O_4 nanoparticles with an inverse spinel structure. The strong and sharp peaks revealed that Fe_3O_4 particles were highly crystallized, which was consistent with the morphologies from the TEM images. The diffraction peak broadening suggested the small size of magnetite nanoparticles. The particle size of the three samples could be estimated from XRD patterns using Scherrer's equation. The calculated crystal grain size of the magnetite nanospheres, nanoneedles and nanocubes was 15.4 nm, 36.8 nm and 51.2 nm, respectively. The sizes of Fe_3O_4 nanoparticles calculated from the XRD patterns were in good agreement with the average sizes determined by TEM images (Fig. 1a, c and e). The accordant results about the size indicated the single crystalline nature of Fe_3O_4 nanoparticles.

3.3. FTIR results

To obtain additional data for characterization of nanospheres, nanoneedles and nanocubes of magnetite, the products were measured by FTIR spectra. The FTIR spectra recorded from 2000 to 500 cm^{-1} of the magnetite nanoparticles obtained at the visible light irradiation time of 30 min are shown in Fig. 3. It was reported that the characteristic absorption band of Fe–O bond of bulk Fe_3O_4 was at 570 cm^{-1} [24]. From Fig. 3, the FTIR spectrum of the magnetite nanospheres, nanoneedles and nanocubes was characterized by a strong absorption band at 606 cm^{-1}, 609 cm^{-1} and 612 cm^{-1}, respectively and no additional peaks. The reason of a small increment in wavenumber is that the surface bond force constant increases with the decrease of particle size to nanoscale dimensions. Therefore, the FTIR spectrum of the three cases exhibited a blue shift and the characteristic absorption band of Fe–O in Fe_3O_4 had a higher wavenumber than that of bulk Fe_3O_4 [25]. These results strongly support to assignment of the contained iron oxide as Fe_3O_4, which suggests that pure magnetite nanospheres, nanoneedles and nanocubes can be prepared at the experimental conditions of this paper.

3.4. Magnetic properties

The magnetic properties of the as-prepared magnetite nanospheres, nanoneedles and nanocubes obtained at visible light irradiation time of 60 min were measured at room temperature, and the magnetic hysteresis (M-H) loops are presented in Fig. 4a–c. From this figure, it was clear that the saturation magnetization of magnetite nanospheres, nanoneedles and nanocubes was 75.9 emu/g (Fig. 4a), 94.2 emu/g (Fig. 4b) and 108.1 emu/g (Fig. 4c). Nanoneedles magnetization is higher that nanospheres, and is close to the theoretical value of bulk Fe_3O_4 (~90 emu/g) [26]. This result indicates the formation of the well-defined crystalline structure for the as-synthesized magnetite nanoparticles. The Fe_3O_4 nanocubes exhibit higher saturation magnetization than that of magnetite nanospheres and nanoneedles, which indicates that the magnetic properties show the shape dependence. In addition, the magnetic behavior of Fe_3O_4 nanoparticles is sensitive to the particle size [27]. It is clearly evident from the TEM images as shown in Fig. 1 that the size of magnetite nanopartilces increases from nanospheres to nanoneedles and to nanocubes. It is well-known that the decrease in particle size can lead to an increasing surface-to-volume ratio, which in turn causes more surface spin disorder, and consequently a reduction in the saturation magnetization [28,29]. The third reason for the increasing saturation magnetization in case of magnetite nanocubes may be related to the increased crystallinity as shown in TEM images of Fig. 1f, comparing with slightly low crystallinity of nanoshperes and nanoneedles as in Fig. 1b and d. Therefore, the increase in the crystallites size from nanospheres to nanoneedles then to

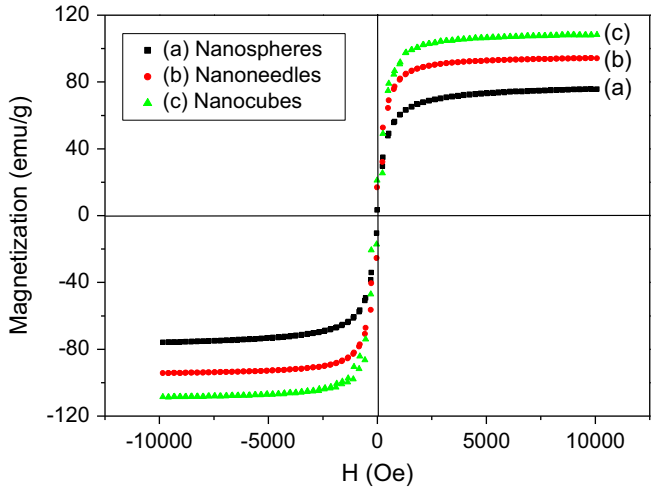

Fig. 4. Magnetic hysteresis loops of (a) nanospheres, (b) nanoneedles and (c) nanocubes of magnetite obtained at the visible light irradiation time of 60 min.

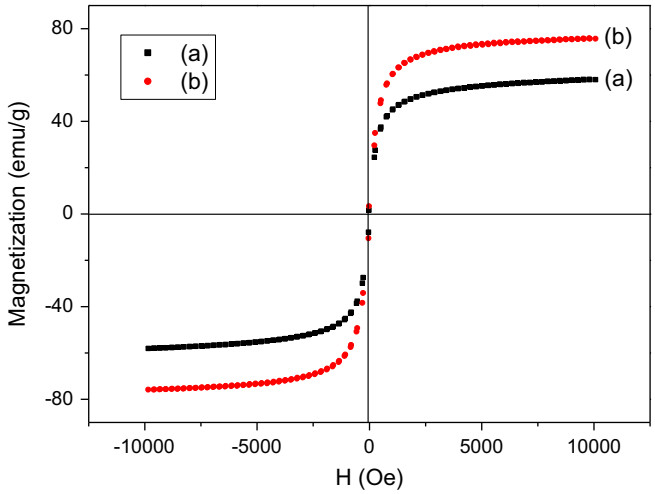

Fig. 5. Magnetic hysteresis loops of magnetite nanospheres obtained at the visible light irradiation time of (a) 30 min and (b) 60 min.

nanocubes of magnetite leads to a corresponding increase in the magnetization value.

In order to illustrate the influence of the particle size on the magnetization value, Figs. 5 and 6 show the magnetite nanospheres and nanocubes synthesized at the visible light irradiation time of 30 min and 60 min, respectively. As seen from Fig. 5, the saturation magnetization of the as-prepared magnetite nanospheres increases from 58.0 emu/g to 75.9 emu/g with the irradiation time of the visible light increased from 30 min to 60 min. The saturation magnetization of the magnetite nanocubes also exhibits an increase to 108.1 emu/g from 97.6 emu/g with the visible light irradiation time increasing from 30 min to 60 min. It was reported that the magnetic anisotropy of the nanoparticles depends on their crystallinity and thus high crystalline structure will cause an increase in the magnetic moment of the nanoparticles [30]. Therefore, the increase in the saturation magnetization may be attributed to the increase in the size and the degree of crystallinity of the magnetite nanoparticles with the irradiation time increasing.

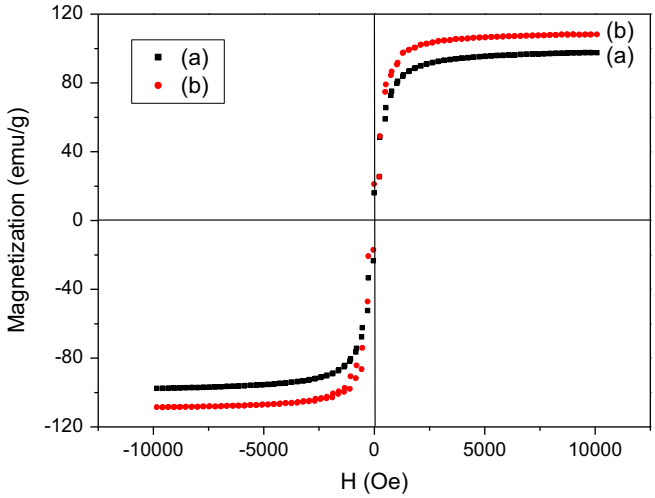

Fig. 6. Magnetic hysteresis loops of magnetite nanocubes obtained at the visible light irradiation time of (a) 30 min and (b) 60 min.

In addition, it was reported that magnetite nanoparticles smaller than approximately 20–30 nm contain a single magnetic domain with a single magnetic moment and exhibit superparamagnetism [31,32]. Therefore, the Fe_3O_4 nanospheres obtained at the visible light irradiation time of 30 min are superparamagnetism at room temperature due to the small particle size of about 15 nm, which is evident from the TEM images as shown in Fig. 1.

4. Conclusions

The shape-controlled magnetite nanoparticles have been successfully prepared via a convenient co-precipitation method. TEM showed that the morphology of magnetite nanoparticles changed from nanospheres to nanoneedles and to nanocubes by varying the amount of SDS. The obtained Fe_3O_4 nanoparticles displayed the perfect regular nanostructure with monodispersion and a narrow distribution in particle size. And the particle size of Fe_3O_4 samples increased with the increase in the visible light irradiation time. From the XRD patterns and FTIR spectra, all shapes of magnetite nanopartilces are pure Fe_3O_4 phase. The Fe_3O_4 nanoparticles exhibited the attractive magnetic properties with high saturation magnetization from the magnetic hysteresis loops. The magnetite nanospheres obtained at the visible light irradiation time of 30 min without SDS are superparamagnetic at room temperature on account of the particle size of about 15 nm, which could be a potential material for the application in biomedicine.

Acknowledgments

The authors are grateful for the supports from the Scientific and Technological Innovation Programs of Higher Education Institutions in Shanxi, China (No. 20121017), the National Natural Science Foundation of China (Nos. 21073113 and 51072105), and the Natural Science Foundation for Young Scientists of Shanxi Province, China (No. 2012021020-5).

References

[1] B.Y. Geng, J.Z. Ma, J.H. You, Controllable synthesis of single-crystalline Fe_3O_4 polyhedra possessing the active basal facets, Crystal Growth and Design 8 (2008) 1443–1447.

[2] L. Cabrera, S. Gutierrez, N. Menendez, M.P. Morales, P. Herrasti, Magnetite nanoparticles: electrochemical synthesis and characterization, Electrochimica Acta 53 (2008) 3436–3441.

[3] W. Wu, Q.G. He, C.Z. Jiang, Magnetic iron oxide nanoparticles: synthesis and surface functionalization strategies, Nanoscale Research Letters 3 (2008) 397–415.

[4] F.H. Chen, L.M. Zhang, Q.T. Chen, Y. Zhang, Z.J. Zhang, Synthesis of a novel magnetic drug delivery system composed of doxorubicin-conjugated Fe_3O_4 nanoparticle cores and a PEG-functionalized porous silica shell, Chemical Communications 46 (2010) 8633–8635.

[5] Y. Chen, H.Y. Chen, D.P. Zeng, Y.B. Tian, F. Chen, J.W. Feng, J.L. Shi, Core/shell structured hollow mesoporous nanocapsules: a potential platform for simultaneous cell imaging and anticancer drug delivery, ACS Nano 4 (2010) 6001–6013.

[6] F.Y. Cheng, C.H. Su, Y.S. Yang, C.S. Yeh, C.Y. Tsai, C.L. Wu, M. T. Wu, D.B. Shieh, Characterization of aqueous dispersions of Fe_3O_4 nanoparticles and their biomedical applications, Biomaterials 26 (2005) 729–738.

[7] S.K. Giri, N.N. Das, G.C. Pradhan, Synthesis and characterization of magnetite nanoparticles using waste iron ore tailings for adsorptive removal of dyes from aqueous solution, Colloids and Surfaces A: Physicochemical and Engineering Aspects 389 (2011) 43–49.

[8] H. Karami, Heavy metal removal from water by magnetite nanorods, Chemical Engineering Journal 219 (2013) 209–216.

[9] J. Kong, J.R. Liu, F.L. Wang, L.Q. Luan, M. Itoh, K. Machida, Electromagnetic wave absorption properties of Fe_3O_4 cubic nanocrystallines in gigahertz range, Applied Physics A: Materials Science and Processing 105 (2011) 351–354.

[10] L.Z. Shen, Y.S. Qiao, Y. Guo, J.R. Tan, Preparation of nanometer-sized black iron oxide pigment by recycling of blast furnace flue dust, Journal of Hazardous Materials 177 (2010) 495–500.

[11] H.W. Wang, H.C. Liu, Y.C. Yeh, Synthesis of Fe_3O_4 nanowire arrays via precipitation in templates and microwave hydrothermal process, International Journal of Applied Ceramic Technology 7 (2010) E33–E38.

[12] A.S. Teja, P.Y. Koh, Synthesis, properties and applications of magnetic iron oxide nanoparticles, Progress in Crystal Growth and Characterization of Materials 55 (2009) 22–45.

[13] M. Abbas, M. Takahashi, C. Kim, Facile sonochemical synthesis of high-moment magnetite (Fe_3O_4) nanocube, Journal of Nanoparticle Research 15 (2013) 1354–1365.

[14] Y. Lee, J. Lee, C. Bae, J. Park, H. Noh, J. Park, T. Hyeon, Large-scale synthesis of uniform and crystalline magnetite nanoparticles using reverse micelles as nanoreactors under reflux conditions, Advanced Functional Materials 15 (2005) 503–509.

[15] T. Togashi, M. Umetsu, T. Naka, S. Ohara, Y. Hatakeyama, T. Adschiri, One-pot hydrothermal synthesis of an assembly of magnetite nanoneedles on a scaffold of cyclic-diphenylalanine nanorods, Journal of Nanoparticle Research 13 (2011) 3991–3999.

[16] M.M. Rashad, H.M. EI-Sayed, M. Rasly, M.I. Nasr, Induction heating studies of magnetite nanospheres synthesized at room temperature for magnetic hyperthermia, Journal of Magnetism and Magnetic Materials 324 (2012) 4019–4023.

[17] G.H. Gao, X.H. Liu, R.R. Shi, K.C. Zhou, Y.G. Shi, R.Z. Ma, T.E. Takayama, G.Z. Qiu, Shape-controlled synthesis and magnetic properties of monodisperse Fe_3O_4 nanocubes, Crystal Growth and Design 10 (2010) 2888–2894.

[18] G.H. Gao, R.R. Shi, W.Q. Qin, Y.G. Shi, G.F. Xu, G.Z. Qiu, X.H. Liu, Solvthermal synthesis and characterization of size-controlled monodisperse Fe_3O_4 nanopartilces, Journal of Materials Science 45 (2010) 3483–3489.

[19] Y.F. Zhu, W.R. Zhao, H.R. Chen, J.L. Shi, A simple one-pot self-assembly route to nanoporous and monodispersed Fe_3O_4 partilces with oriented attachment structure and magnetic property, Journal of Physical Chemistry C 111 (2007) 5281–5285.

[20] K. Petcharoen, A. Sirivat, Synthesis and characterization of magnetite nanoparticles via the chemical co-precipitation method, Materials Science and Engineering B: Advanced Functional Solid-State Materials 177 (2012) 421–427.

[21] X. Zhou, Y.F. Shi, L. Ren, S.X. Bao, Y. Han, S.C. Wu, H.G. Zhang, L.B. Zhong, Q.Q. Zhang, Controllable synthesis, magnetic and biocompatible properties of Fe_3O_4 and α-Fe_2O_3 nanocrystals, Journal of Solid State Chemistry 196 (2012) 138–144.

[22] Y.Y. Zheng, X.B. Wang, L. Shang, C.R. Li, C. Cui, W.J. Dong, W.H. Tang, B.Y. Chen, Fabrication of shape controlled Fe_3O_4 nanostructure, Materials Characterization 61 (2010) 489–492.

[23] K. Aslam, Preparation and characterization of magnetic nanoparticles embedded in microgels, Materials Letters 62 (2008) 898–902.

[24] R.M. Cornell, U. Schwertmann, The Iron Oxides, second ed., Wiley-VCH Verlag GmbH & Co., KGaA, Weinheim, 2003.

[25] M. Ma, Y. Zhang, W. Yu, H.Y. Shen, H.Q. Zhang, N. Gu, Preparation and characterization of magnetite nanoparticles coated by amino silane, Colloids and Surfaces A: Physicochemical and Engineering Aspects 212 (2003) 219–226.

[26] D.E. Zhang, X.J. Zhang, X.M. Ni, J.M. Song, H.G. Zheng, Fabrication and characterization of Fe_3O_4 octahedrons via an EDTA-assisted route, Crystal Growth and Design 7 (2007) 2117–2119.

[27] K.Y. Yoon, C. Kotsmar, D.R. Ingram, C. Huh, S.L. Bryant, T.E. Milner, K.P. Johnston, Stabilization of superparamagnetic iron oxide nanoclusters in concentrated brine with cross-linked polymer shells, Langmuir 27 (2011) 10962–10969.

[28] M. Rajendran, R.C. Pullar, A.K. Bhattacharya, D. Das, S.N. Chintalapudi, C.K. Majumdar, Magnetic properties of nanocrystalline $CoFe_2O_4$ powders prepared at room temperature: variation with crystalline size, Journal of Magnetism and Magnetic Materials 232 (2001) 71–83.

[29] S. Roy, I. Dubenko, D.D. Edorth, N. Ali, Size induced variations in structural and magnetic properties of double exchange $Ls_{0.8}Sr_{0.2}MnO_{3-\delta}$ nano-ferromagnet, Journal of Applied Physics 96 (2004) 1202–1208.

[30] R.P. Patil, P.P. Hankare, K.M. Garadkar, R. Sasikala, Effect of sintering temperature on structural, magnetic properties of lithium chromium ferrite, Journal of Alloys and Compounds 523 (2012) 66–71.

[31] S.R. Dave, X. Gao, Monodisperse magnetic nanoparticles for biodetection, imaging, and drug delivery: a versatile and evolving technology, Wiley Interdisciplinary Reviews: Nanomedicine and Nanobiotechnology 1 (2009) 583–609.

[32] J.Y. Jing, Y. Zhang, J.Y. Liang, Q.B. Zhang, E. Bryant, C. Avendano, V.L. Colvin, Y.D. Wang, W.Y. Li, W.W. Yu, One-step reverse precipitation synthesis of water-dispersible superparamagnetic magnetite nanoparticles, Journal of Nanoparticle Research 14 (2012) 827–834.